# D3.3

# DEVELOPMENT OF A NEW EXPERIMENTAL BENCH DEDICATED TO OBLIQUE CUTTING MONITORING

AUTHOR:

ESR7
HAYTHEM
ZOUABI

This project received funding from the European Union's Marie Skłodowska-Curie Actions (MSCA) Innovative Training Networks (ITN) H2020-MSCA-ITN-2017 under the grant agreement N°764979

## Content

# 1. Introduction

This deliverable 3.3 "Development of new experimental instrumented bench dedicated to orthogonal, oblique cutting and intense friction tests monitoring" is the second deliverable in the WP3. In the first one: "Setting up Standard Test cases for the Studied Processes", the standard test cases were defined and thus, this document is set to describe mainly the functional specification of the bench that is required to meet our needs in term of measurement accuracy with respect to the operating cutting parameters fixed in the deliverable 3.1.
The following section describe the developed benches in the literature for cutting and friction investigation and the specifications of each one.

# 2. State of the art

## 2.1 Orthogonal/Oblique instrumented cutting benches

### 2.1.1 Linear benches

In linear benches, experiments are conducted with a linear movement of the workpiece in front of the fixed tool.
[Sutter, 1998] described the Hopkinson bar device which was designed to perform orthogonal cutting tests in a wide range of cutting velocities. [Figure 1] describe the configuration. Two tools are symmetrically mounted on the tool holding fixture. The workpiece is carried by the projectile which is launched by an air gun. Minimal cutting speed of this bench is 0.6m/min [Molinari, 2002].

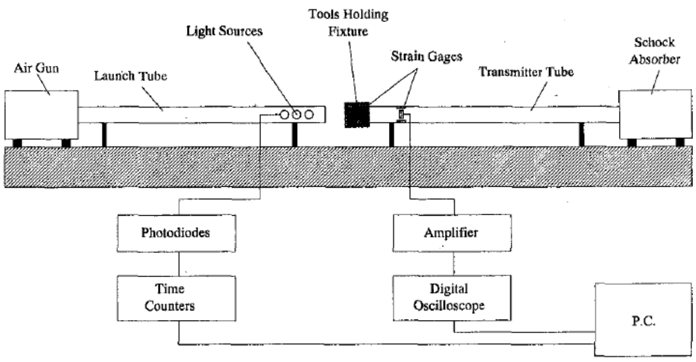


Figure 1: Configuration of the high speed machining device "Hopkinson bar", [Sutter, 1998].

Orthogonal cutting tests with different rake angles and oblique cutting can be experienced by changing the tool holding fixture.

[Molinari, 2002] studied the geometrical characteristics of the adiabatic shear bands (band width, band spacing) and the segmentation frequency of Ti-6Al-4V with [0.01, 73m/s] as the range of cutting velocities.
[Sutter, 2003] used the Hopkinson bar device with intensified CCD camera for temperature investigation on the side view including the primary shear zone and the tool-chip contact.

On the other hand, [Guo, 2015] used a tensile/compression test machine for cutting. The experimental device [Figure 2] mounted on the machine consists of a die block and a die cover with an imaging window for kinematic fields measurements. The workpiece is held inside the vertical channel and the tool is held and fixed inside the horizontal channel. Test were performed on single-phase 70-30 brass with a cutting speed equal to 1m/s.

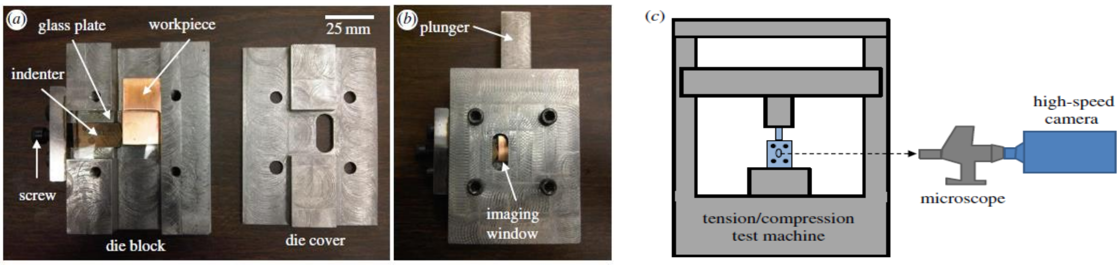


Figure 2: Cutting and friction tests on tensile/ compression test machine, [Guo, 2015].

[Pottier, 2014] used a planer machine [Figure 3] to perform instrumented orthogonal cutting tests on Ti-6Al-4V rectangular specimen which was held to the machine table. 6m/min was the experienced cutting speed.

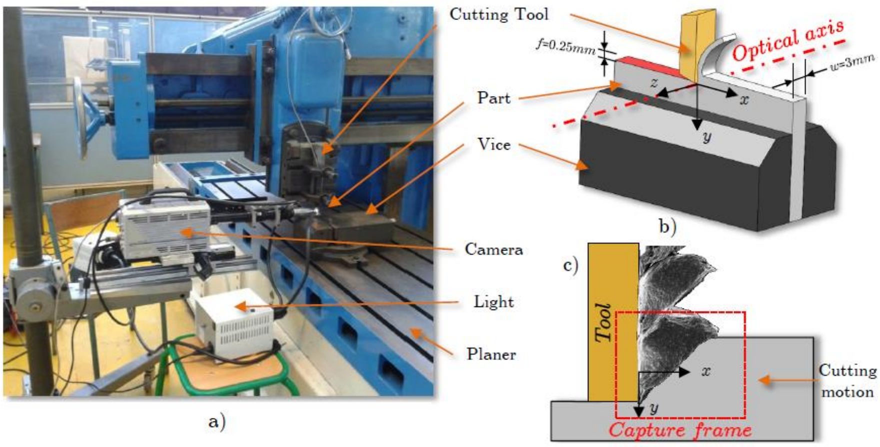


Figure 3: a) Experimental apparatus, b) cutting configuration c) side view of the scene, [Pottier, 2014].

Recently, [Harzallah, 2018] used the milling machine' table to monitor orthogonal cutting tests on Ti-6Al-4V. The movement of the specimens was ensured by a linear shaft and electric motor [Figure, 4]. The experienced cutting speeds were 3 and 15m/min with 0° and 15° for the rake angles. Based on the work of [Whitenton, 2010], he developed a coupled visual and thermal imaging device named VISIR [Figure 4]. A visual image and thermal image can be recorded synchronously. The main objective behind instrumented experimentation was to establish a local energy balance. The energy contribution of each zone was quantified. Experimental data about stresses in shear zones, chip sliding velocities and temperature fields were used for this purpose.

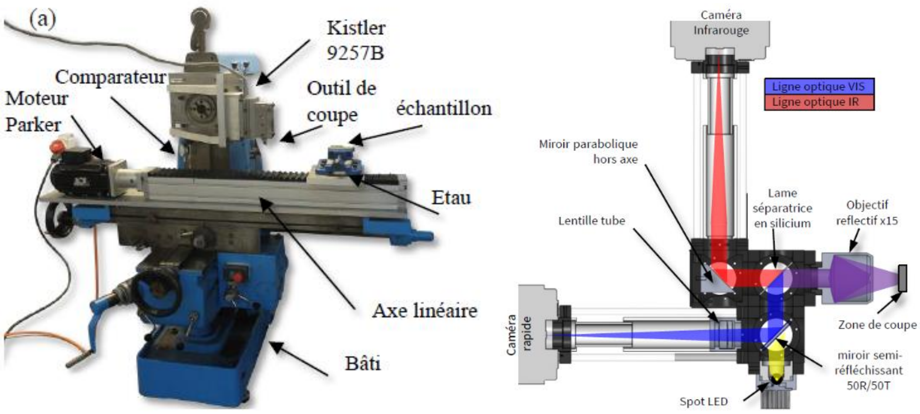


Figure 4: a) Orthogonal cutting bench, b) The VISIR device [Harzallah, 2018].

[Thimm, 2018] developed a newly experimental bench [Figure 5] capable to undergo orthogonal cutting tests with a linear movement of the workpiece at a maximum speed of 240m/min. Instrumented experiment was performed on Aisi 1045 at a cutting speed of 125m/min and 0.1mm as depth of cut.

Figure 5: The newly developed bench for orthogonal cutting experiments in [Thimm, 2018].

### 2.1.2 Rotated benches

- Instrumented Cutting tests on tubes

[Bothroyd, 1961] used tubes to conduct experiments on carbon steel with infrared camera imaging the side surface of the workpiece, tool and chip. Furthermore, [Dinc, 2008] performed orthogonal cutting tests using a vertical CNC milling machine where the workpiece was held in the tool holder on the spindle [Figure 7]. The experienced cutting speeds were 160m/min and 200m/min for the Al7075 and 40m/min, 60m/min and 80m/min for Aisi1050.

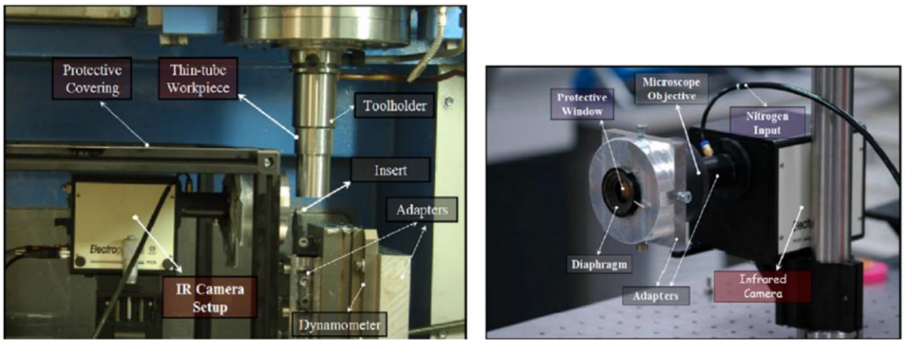


a) b)

Figure 7: a) Vertical CNC milling machine used for instrumented orthogonal cutting tests, b) IR camera system for temperature measurement in [Dinc, 2008].

In the same context and for temperature investigation, [Soler, 2015] performed experimental tests on samples of different titanium alloys in form of cylindrical tubes. The samples were held in a Lagun HS 1000 vertical CNC machining center which controlled the cutting conditions. [Soler, 2018] used the same experimental bench with tube containing slots: During the test, the tool heats up. When the tool reaches the slot, a thermal image of the tool rake face could be captured. Tests were conducted on Aisi 4140 with a cutting speed of 250m/min. The schematic description of the experimental configuration is given in [Figure 6].

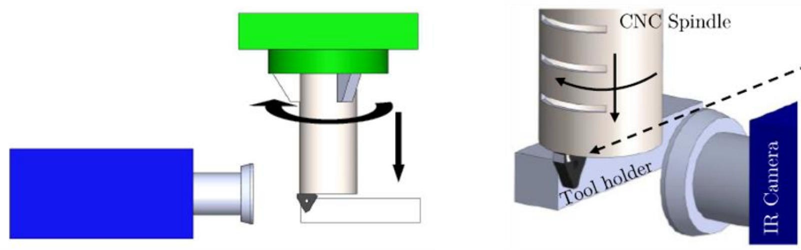


a) b)

Figure 6: Experimental apparatus: a) Configuration [Soler, 2015], b) instrumented orthogonal cutting test on tube containing slots, [Soler, 2018].

[Bouchnak, 2010] developed an experimental bench to monitor orthogonal cutting tests on Ti555-3 Tubes. The bench [Figure 8] was equipped with 2 infrared cameras. The first, placed horizontally, imaged the side view of the workpiece, chip and tool. The second, placed vertically, imaged the upper surface of the chip.

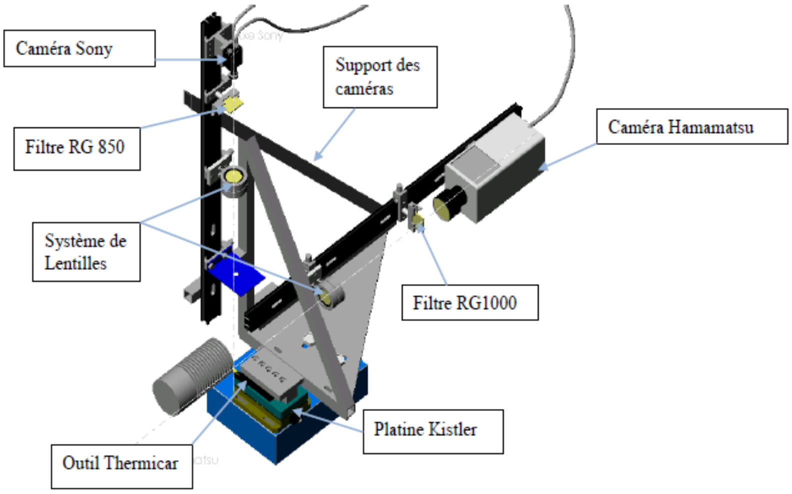


Figure 8: Developed bench in [Bouchnak, 2010].

## ➢ Instrumented Cutting tests on disks

Force data, tool-chip contact length, chip segment geometry, shear strain, chip segmentation angles and chip segmentation frequency of Ti-6Al-4V were studied in [Cotterell, 2008a and b] with a range of cutting speeds varying from 4m/min to 120m/min. Disks with 2 mm of thickness were held in the mandrel of the lathe machine [Figure 9.a]. Visual images were recorded using a high-speed camera [Figure 9.b] with 24000 frame/s and at a resolution of 512 * 128 pixels.

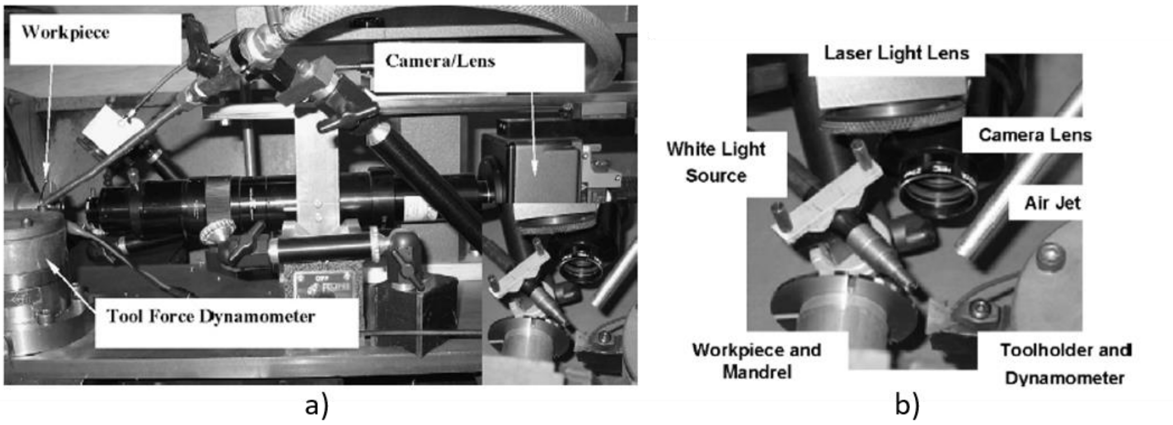


Figure 9: a) Experimental apparatus with close up of tool/workpiece arrangement [Cotterell, 2008a]; b) Set up of visual imaging system [Cotterell, 2008b].

[Heigel, 2017] used a transparent YAG tool to measure the temperature at the tool-chip interface. Experiments were carried out through orthogonal cutting tests on Ti-6Al-4V disks with 100mm of diameter and 1mm of thickness. The cutting speeds were from 20m/min to 100m/min with 20m/min as increment. Thermal images were recorded using an IR camera with a rate of 700Hz, so the resolution was 160*120 pixels.

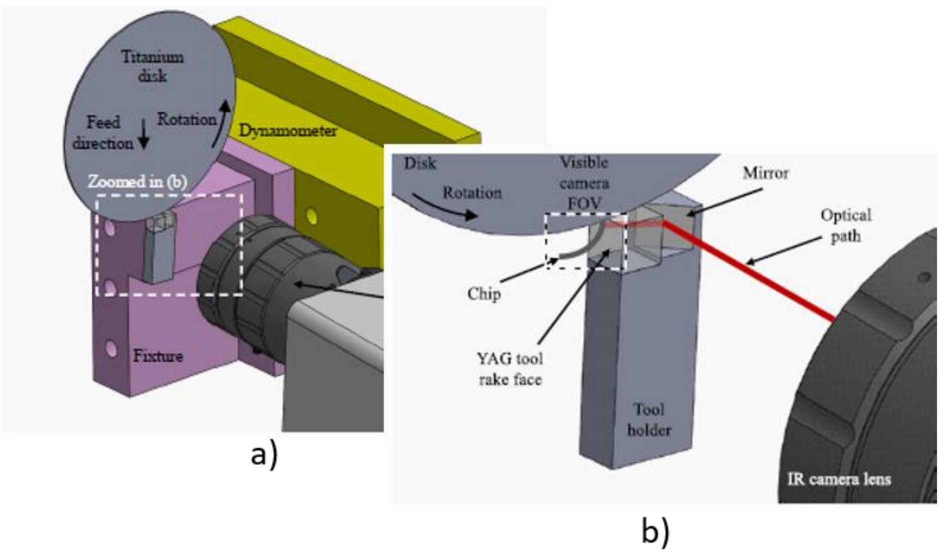


Figure 10: The experiment set up to measure the tool-chip interface temperature: a) The measurement set up; b) Zoomed in, [Heigel, 2017].

## 2.2 Friction benches

Friction properties at the tool/chip/workpiece interface in dry machining of AISI 4140 steel were studied in the developed tribometer [Figure 11] described in [Claudin, 2008]. A pin slide on a refreshed surface of the rotated cylindrical workpiece. The influence of the contact pressure was studied through tests with different diameters of the pin. The pneumatic jack consists on applying the contact pressure. Helical path showed in [Figure 11] was generated by both the feed provided to the pin and rotation of the workpiece. This experimental device was mounted on a lathe to ensure sufficient sliding velocities. The pin was held in the pin-holder equipped with a thermistor to provide data about instantaneous heat flux entering into the pin. Also, the pin-holder was mounted in a dynamometer to provide the apparent normal and tangential force. The contact pressure and the sliding velocity were chosen with respect to the frictional conditions along the tool/chip/Workpiece interfaces: The sliding velocity at the rake face (Tool/chip interface) and the sliding velocity at the flank face (Tool/Workpiece interface).
Experiments on AISI 4140 were carried out using sliding speeds of {60, 90, 120, 150, 200m/min}. A normal force of 1000N was applied to the pin which has a diameter of 9mm that gives a contact pressure of about 2600MPa.

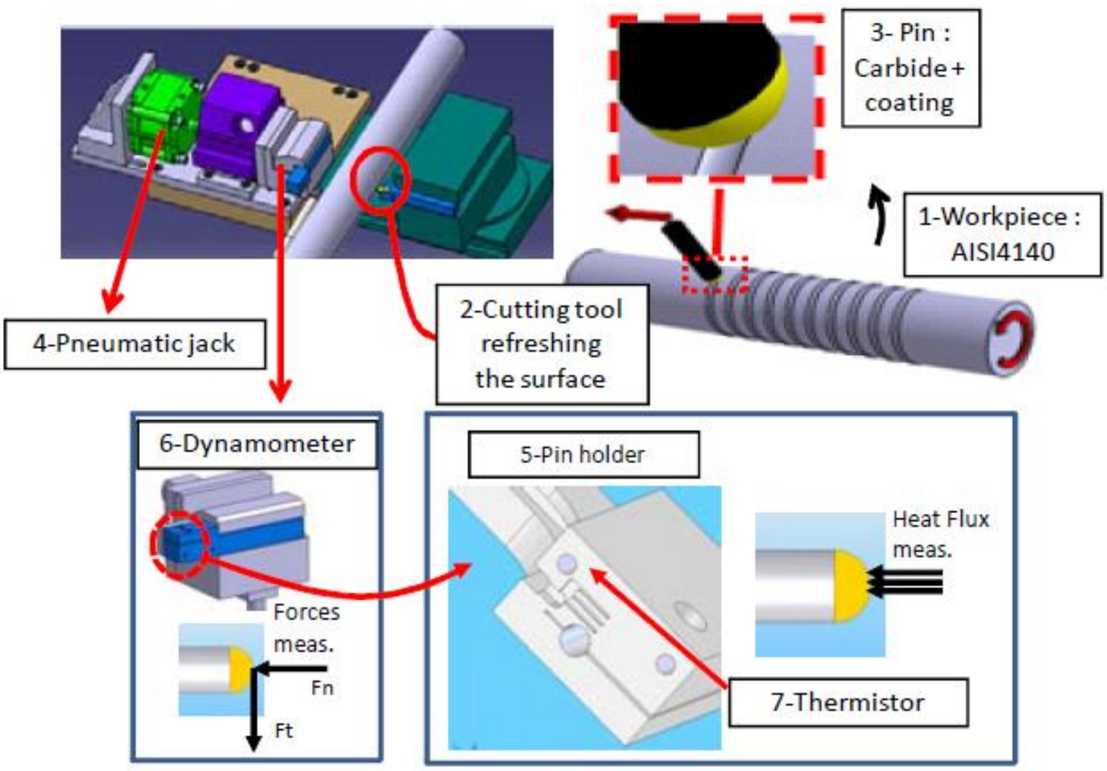


Figure 11: Set up of the tribometer device, [Claudin, 2008].

[Puls, 2013] used a vertical broaching machine [Figure 12] to monitor experimental investigation on friction under metal cutting conditions. The maximum cutting speed is of 100m/min. Experimental tests were made to analyze friction experienced at the tool-chip interface. The tool was mounted on a tool holding device which is also mounted on a Kistler dynamometer using a base plate. The bench is derived from orthogonal cutting benches. It was used to perform friction tests. To avoid chip formation, he adjusted a negative rake angle. The experienced rake angles were -7° and -10°. As a result, it leads to plastic flow of the workpiece metal. According to [Puls, 2014], such conditions will generates high contact temperatures which matches with the conditions experienced in metal cutting. Experiments were made on three materials: AISI 1045, AISI 4140 and Inconel 718.

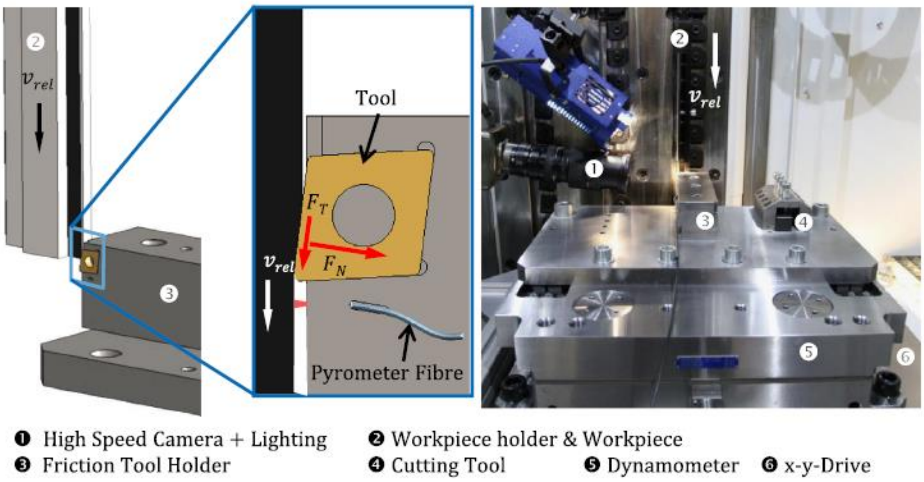

Figure 12: Test bench design for friction investigation under cutting conditions and experimental set up, [Puls, 2014].

[Grzesik, 2014] measured the friction coefficient in turning configuration. Cutting speeds of {100, 160, 240, 320, 400, 480} were used with a negative rake angle of -6°. Friction models for both orthogonal and oblique cutting was deduced from modeling of friction in oblique cutting configuration. A transformation of componential forces was done [Figure 13].

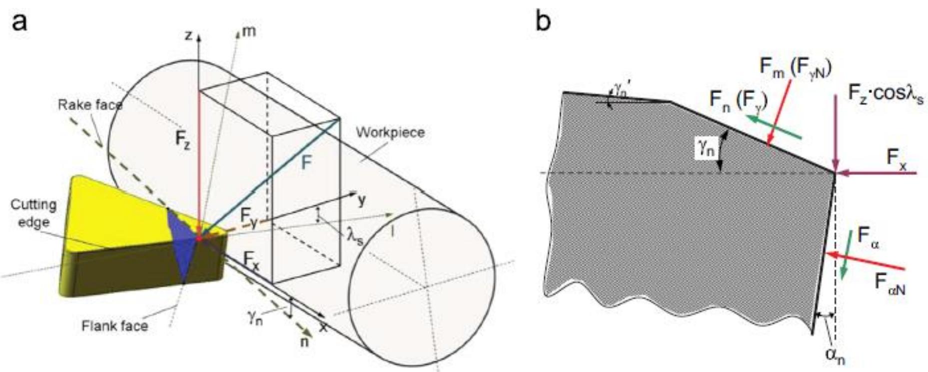

Figure 13: a) Localization of various coordinate systems; b) acting forces, [Grzesik, 2014].

[Grzesik, 2014] noted the change of friction and normal forces acting on both the flank and rake face with the progress of wear. He traced back this point to the generated differences in increments of cutting forces when varying the cutting speed. Using the friction models, he described the evolution of the friction coefficient function of the cutting speeds ranged in {100, 160, 240, 320, 400, 480m/min}. Friction experienced in wear tests were extended by the Cylinder-on-disK device. The schematic apparatus of the device' configuration is given by the following figure:

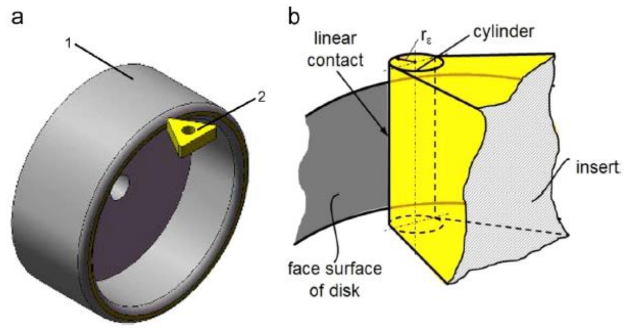

Figure 14: a) General view and b) Scheme of the contact between the inset and disk, [Grzesik, 2014].

Friction test were conducted with 160m/min and 240m/min as a sliding speeds and with {50, 75, 100N} as the range of normal load. Results showed that the friction coefficient is sensitive to both the sliding velocity and normal load: It increases with decreasing of the sliding velocity or the normal load.

Furthermore, [Meier, 2017] designed a tribometer for friction investigation [Figure 15] and which was described also in [Grzesik, 2019]. It was used on a lathe machine. It consists of a cutting tool and a pin which is pressed against the refreshed cutting surface. A piezo-electric sensor is used to measure the force components acting to the pin. Distance between the pin and the tool was chosen with respect to the time delay that do not lead to significant oxidation which in general change the frictional properties of a surface. Friction tests were made on Ti-6Al-4V with a range of cutting speeds varying from 10m/min to 100m/min. The evolution of the coefficient of friction function of velocities was compared to the results of two other type of tribometer: The Pin-on-disk tribometer and the Spiral pin-on-disk tribometer.

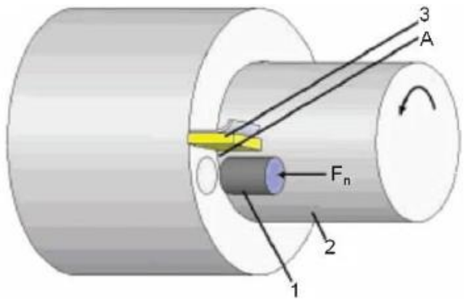

1 – pin, 2 – workpiece, 3 – cutting insert,
A – contact zone

Figure 15: Schematic apparatus of the tribometer [Grzesik and Rech, 2019].

## 2.3 Conclusion

To summarize, this section gives a review on the previously developed experimental benches for cutting and friction investigation. The main points which were discussed are:

- Cutting and sliding speeds experienced on the bench.
- Tested materials on the bench.
- Measurements: force data, temperature and kinematic fields and friction coefficient.

Different cutting and friction configurations were described in order to study:

- Kinematic fields measurement at the side view.
- Temperature measurement at the side view.
- Temperature prediction at the tool-chip interface.
- Friction coefficient measurement under cutting conditions: How to reproduce cutting conditions in order to monitor friction investigation at the tool-chip interface.

UNIVERSITY OF BORDEAUX

# Functional Specifications

## Experimental Bench for temperature and kinematic fields measurement during orthogonal cutting and friction tests.

<u>Date</u>: 22/03/2019.
<u>Topic</u>: Functional specifications of the experimental bench for temperature and kinematic fields measurement during orthogonal cutting and friction tests.

<u>Author</u>: Haythem ZOUABI.

# 3. Functional Specifications

## 3.1 Context

In order to improve the thermomechanical and tribological behavior laws, the use of instrumented cutting or friction tests is necessary.
This bench must therefore make it possible to:

- Carry out instrumented orthogonal/Oblique cutting tests and,
- Instrumented friction tests.

## 3.2 Materials

In the framework of the ENABLE project, experiments will be made on the following materials:

- Ti-6Al-4V
- Inconel 718.
- Aeronautical aluminum alloy: Al7075.

## 3.3 Kinematic scheme of the bench

The following refers to:

0: Bench' bed.

1: Set {Piece, Vise}.

2: Axis.

3: Support.

4: Set {Tool holder, Tool}.

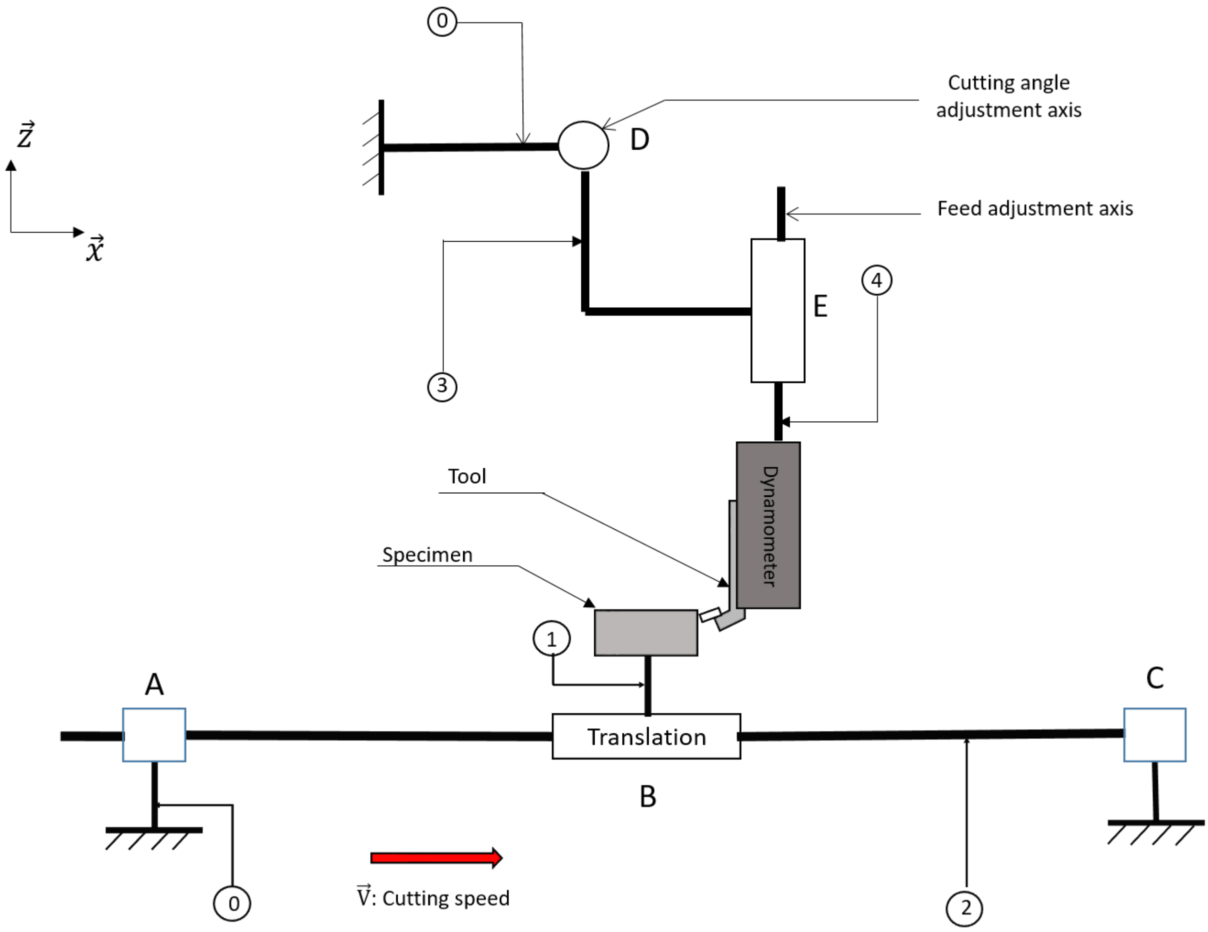


Figure 16: Kinematic scheme of the Bench.

The specimen will be driven by a translation movement at a speed V, along $x_+$ and in front of the tool which is held fixed. The return of the specimen to its initial position must be done without contact with the tool.

To allow positioning the specimen in front of the tool, two solutions could be anticipated:

- The set {0, 1 and 2} could be mounted on a table that can moves along the $\vec{y}$ axis.
- The tool-holder can translate along the $\vec{y}$ axis.

This bench must first integrate instruments for measuring the displacement in the table of 1200 mm length as well as its movement speed and measurement of rotation angle of the tool holder.

## 3.4 Technical requirements in terms of:

### 3.4.1 Shape and size of samples

The samples have a rectangular shape. Table 1 summarizes the dimensions of samples planned for this study. These samples will be moved in translation in front of the tool which must be fixed to a specific vertical and angular position. In our test case, the cutting angles are between 0 ° and 6 °.

| | L (mm) | l (mm) | e (mm) | Volume ($mm^3$) |
|---|---|---|---|---|
| **Rectangular 1 (Cut)** | 100 | 60 | 3 | $18.10^3$ |
| **Rectangular 2 (Friction)** | 400 | 60 | 50 | $1200.10^3$ |

Table 1: Dimensional characteristics of samples.

### 3.4.2 Speeds and accelerations

Orthogonal cutting or friction tests will be performed with cutting speeds ranging from 5m/min to 80m/min. The translation speed of the table must always be kept constant over a distance of 400mm minimum.

### 3.4.3 Efforts to bear

- Cutting tests: $\vec{x}$ is the direction of sample' translation and $\vec{z}$ the tap direction. The orthogonal cutting tests on the titanium alloy Ti-6Al-4V at 3m/min and with a rake angle of 0° generates a cutting force $F_x$ = 1600N with fluctuations that do not exceed +200N and -500N [Harzallah, 2018]. Thus, it is estimated that the bench will have to withstand maximal forces of:

  - $F_x = 2000N$, [Harzallah, 2018].
  - $F_z = 1500N$, [Fang, 2009].

[Fang, 2009] presented results about the force ratio between the cutting and the thrust forces. With a cutting speed of 50m/min and a depth of cut of 0,12mm/tr, the force ratio doesn't exceed 1,3.
In the same work, [Fang, 2009] presented the normalized cutting forces recorded when cutting the Inconel 718 with a range of cutting speeds which belong to [50…180m/min]. It showed that the maximum cutting forces doesn't exceed the cutting forces of Ti-6Al-4V with a low cutting speed of 3m/min.
Cutting forces of Al7075 is obviously much lower due to its lower hardness (105HV).

- Friction tests: $\vec{x}$ is the direction of the specimen' translation and $\vec{z}$ is the tap direction.

[Nouari, 2008] conducted cutting tests on Ti-6Al-4V for friction and wear investigation. He noted an increase in the cutting forces at the end of the test compared with the beginning. It was related to the wear evolution during the friction test. Table 2 summarizes the relevant data during experiments function of the cutting conditions.

| Test | $V_c$ (m/min) | α° | f(mm) | $F_c$ beginning (N) | $F_c$ End (N) | $F_f$ beginning (N) | $F_f$ end (N) | µ begenning | µ end |
|---|---|---|---|---|---|---|---|---|---|
| 1 | 15 | 0 | 0.1 | 900 | 1100 | 400 | 480 | 0.44 | 0.43 |
| 2 | 15 | 0 | 0.2 | 1200 | 1350 | 520 | 600 | 0.43 | 0.44 |
| 3 | 15 | 0 | 0.3 | 1750 | 2100 | 700 | 850 | 0.4 | 0.4 |
| 4 | 30 | 0 | 0.1 | 970 | 1200 | 450 | 550 | 0.46 | 0.46 |
| 5 | 30 | 0 | 0.2 | 1250 | 1420 | 580 | 1200 | 0.46 | 0.85 |
| 6 | 30 | 0 | 0.3 | 1300 | 1790 | 420 | 700 | 0.32 | 0.39 |
| 7 | 60 | 0 | 0.1 | 800 | 1000 | 300 | 600 | 0.37 | 0.6 |
| 8 | 60 | 0 | 0.2 | 900 | 1100 | 580 | 710 | 0.64 | 0.65 |
| 9 | 60 | 0 | 0.3 | 1600 | 1950 | 800 | 1170 | 0.5 | 0.6 |
| 10 | 15 | 30 | 0.1 | 450 | 600 | 60 | 50 | 0.77 | 0.7 |

Table 2: Evolution of the cutting forces and the friction coefficient function of the cutting conditions during experiments on Ti-6Al-4V, [Nouari, 2008].

Results of friction tests on Inconel 718 with a depth of cut of 0,5mm and a tool rake angle of 10° are described in [Puls, 2014]. The following table presented the evolution ranges of the normal and tangential stresses function of the sliding speeds.

| Sliding speeds | Normal stress | Tangential stress |
|---|---|---|
| [20..100m/min] | [1400..1600 MPa] | [200..500 MPa] |

Table 3: Evolution of the normal and tangential stresses function of the sliding speeds, [Puls, 2014].

[Meier, 2017] conducted friction tests using disks of Ti-6A-4V. The tool and the pin is in contact with the machined surface. A piezoelectric sensor is used to measure the force components. The following table summarizes the variation of the coefficient of friction as a function of the speeds of rotation and according to the intensity of the pre-loading applied:

| Vitesse (m/min) | Effort normal (N) | Coefficient de frottement |
|---|---|---|
| 10--->100 | **100** | 0,45-0,5 |
| 20--->100 | **400** | ≈0,3 |

Table 4: Coefficient of friction versus velocities and pre-loading applied in Ti-6Al-4V pion-disk tests, [Meier, 2017].

### 3.4.4 Instrumentations

- Measurement of the generated forces

The expected range of cutting forces to be measured during tests on both materials can be estimated by:

- $F_x \in [315, 1600N]$ [Fang, 2009 ; Harzallah, 2018].
- $F_z \in [300, 804{,}5N]$ [Fang, 2009 ; Wang, 2015].

To measure the force components acting on the tool, this must be equipped with a dynamometer which its surface is indicaed in table3. The tool-holder will be mounted on this dynamometer.

| | **P. des efforts (KN)** | **Frequency (KHz) *** | | **Mounted surface (mm²)** | **Rigidity (N/µm)** | **Weight (Kg)** |
|---|---|---|---|---|---|---|
| **KISTLER 9129AA** | -10…10 | $F_n(x)=3{,}5$<br>$F_n(y)=4{,}5$<br>$F_n(z)=3{,}5$<br>Mounting on a rigid base | $F_n(x)=1{,}5$<br>$F_n(y)=1{,}5$<br>$F_n(z)=2{,}5$<br>Mounting with machine adapter (CNC) | 90*105 | $c_x=c_z=1000$<br>$c_y=4000$ | Dynamometer : 3,2<br>Plaque de couverture : 2 |

Table 5: Dimensional and functional characteristics of the KISTLER 9129AA dynamometer.

- Kinematic field measurement

The use of a high-speed camera requires a lighting system directed to the viewing scene. This bench must allow placing the instruments in front of the side view.

Dimensions of ones of the expected to use instruments are given in the following tables.

| | Dimensions | Weight |
|---|---|---|
| **OLYMPUS ILP1** | 166 mm (L) × 109 mm (H) × 261mm (P) | 2,9 kg |

Table 6: Dimensions of the OLYMPUS ILP1 lighting system.

| | Dimensions | Poids |
|---|---|---|
| **FASTCAM SA5** | 165 mm × 153 mm × 242,5mm | 6,2 Kg |

Table 7: Dimensions of the high-speed camera FASTCAM SA5.

- Thermal field measurement

An infrared camera will be used for the measurement of the thermal field during the tests. The temperature range of the tests is between 100°C and 1000°C.

This bench must guarantee the minimum of space to be able to place the cameras on both sides of the lateral surface of the specimen. The cameras will be positioned perpendicular to the viewing scene (lateral surface of the specimen) and thus in the direction of the y axis.

### 3.4.5 Bench Axes

- Axes and number of axes

The following refers to

- X: Axis of displacement of the specimens.
- Y: Positioning axis of the specimen in front of the tool.
- Z: Axis to adjust the depth of cut.
- B: Rotation around $\vec{y}$/ Axis to adjust the cutting angle.

Thus, the bench has:

- Operating axis: $\vec{x}$.
- Depth adjustment axis: $\vec{z}$.
- Cutting angle adjustment axis: Rotation along the $\vec{y}$axis.
- Axis of positioning of the specimen in front of the tool: Translation along $\vec{y}$.

### 3.4.6 Rigidity of the bench

To meet our needs in term of measurement accuracy, we have to carry out about rigidities of the bench. Precisions that we are looking for will be converted into criteria of rigidity.

We are looking for great precision in terms of:
- Depth of cut kept constant.
- Cutting angle kept constant.
- Cutting speed kept constant.

The rigidity criteria [Table 6] that derive from these points:
- Criterion in maximum arrow.
- Criterion in maximum relative displacement of the tip of the tool relative to the speciemen.
- Deflection angle criterion of the {Tool Holder, Tool} set.

The maximum allowable displacements along the axes of the bench as well as the associated rigidities are given in the following table; i = {x, y, z}.

| Axes | $\vec{x}$ | $\vec{y}$ | $\vec{z}$ |
|---|---|---|---|
| Displacement $\Delta L_{i,max}$(µm) | 5 | 5 | 5 |
| Rigidity (N/µm) | >400 | --- | >300 |

Table 8: Criteria in terms of maximum authorized movements as well as the associated rigidities.

## 3.5 Environmental conditions

The test bench is intended to be placed in a workshop where the room temperature can vary between 15°C and 40°C.

## 3.6 Safety and maintenance

- Electrical safety with to respect to standards.
- Cowling according to safety standards and access to the visualization scene.
- Emergency stops:
  - Manual stop button.
  - Automatic stop in case the force generated during the cutting or friction tests exceeds the limit force to be borne by the bench.
- Minimum maintenance: Qualification and moments of intervention.

# 4. Meeting and discussions with members of the TechnoShop

The design of the bench will be the result of a cooperative work with TechnoShop. On Tuesday 02/04/2019, I have met Joffrey SARAZIN, Engineer in Mechanical design to TechnoShop and we discussed about the bench specifications through the following points:

- Principles of the bench.
- Dimensions of test samples.

- Range of speeds to experiment and the contraints on it.
- Instrumentation relating to the bench.
- Efforts to be supported by the bench.
- Kinematics of the bench.
- The operating axis and the adjustment ones.
- Rigidity.
- Obstruction and accessibility to the scene of visualization by high-speed and thermal camera.
- Automatic stop in the case of exceeded effort.

# 5. Conclusion

Technologies of different developed orthogonal\oblique cutting benches and tribometers were described. Different experimental configurations were presented function of the measured data and/or the field of view. Cutting conditions and reproduced cutting conditions for the case of friction investigation were discussed in this document.
To meet our needs in term of measurement accuracy, functional specifications was studied and approved with respect to the standard test cases mentioned in the deliverable 3.1. The development of the bench will be the result of a cooperative work with the TechnoShop I.U.T Bordeaux.

# 6. *References*


T.B. **Bouchnak**, *Etude du comportement en sollicitations extrêmes et de l'usinabilite d'un nouvel alliage de titane aéronautique : le ti555-3,* PhD Thesis, Ecole Nationale Supérieure d'Arts et Métiers, Angers, 2010.

G. **Boothroyd**, 1961, *Photographic technique for the determination of metal cutting temperatures*, BRITISH JOURNAL OF APPLIED PHYSICS, Vol 12.

C. **Claudin**, J. Rech, W. Grzesik, S. Zalisz , 2008, *Characterization of the friction properties of various coatings at the tool–chip–workpiece interfaces in dry machining of AISI 4140 steel,* International Journal of Material Forming.

M. **Cotterell**, G. Byrne, 2008a, *Characterisation of chip formation during orthogonal cutting of titanium alloy Ti–6Al–4V*, CIRP Journal of Manufacturing Science and Technology, 41(7):1055-1070.

M. **Cotterell**, G. Byrne, 2008b, *Dynamics of chip formation during orthogonal cutting of titanium alloy Ti–6Al–4V*, CIRP Annals - Manufacturing Technology 57: 93–96.

C. **Dinc**, I. Lazoglu, A. Serpenguzel, 2008, *Analysis of thermal fields in orthogonal machining with infrared imaging*, journal of materials processing technology, 198: 147-154.

N. **Fang**, Q. Wu, 2009, *A comparative study of the cutting forces in high speed machining of Ti–6Al–4V and Inconel 718 with a round cutting edge tool*, Journal of Materials Processing Technology, 209 : 4385-4389.

M. **Harzallah**, *Caractérisation in-situ et modélisation des mécanismes et couplages thermomécaniques en usinage-Application à l'alliage de titane Ti-6Al-4V*, PhD thesis, Université de Toulouse, 2018.

J.C. **Heigel**, E. Whitenton, B. Lane, M.A. Donmez, V. Madhavan, W. Moscoso-Kingsley, 2017, Infrared Measurement of the Temperature at the Tool-Chip Interface While Machining Ti-6Al-4V, Journal of Materials Processing Technology.

W. **Grzesik**, J. Rech, K. Zak, 2014, *Determination of friction in metal cutting with tool wear and flank face effects*, Journal of wear, 317 : 8-16.

W. **Grzesik**, J. Rech, 2019, *Methods and devices for measuring metal cutting friction and wear.*

Y. **Guo**, W.D. Compton, S. Chandraskar, 2015, *In situ analysis of flow dynamics and deformation fields in cutting and sliding of metals.*

L. **Meier**, N. Schaal, K. Wegener, 2017, *In-process measurement of the coefficient of friction on titani*um, 16th CIRP Conference on Modelling of Machining Operations, 58: 163 – 168.

A. **Molinari**, C. Musquar, G. Sutter, 2002, *Adiabatic shear banding in high speed machining of Ti–6Al–4V: experiments and modeling,* International journal of plasticity, 18: 443-459.

M. **Nouari**, M. Calamaz, F. Girot, 2008, *Mécanismes d'usure des outils coupants en usinage à sec de l'alliage,* C. R. Mecanique, 336 : 772-781.

de titane aéronautique Ti–6Al–4V

T. **Pottier**, G. Germain, M. Calamaz, A. Morel, D. Coupard, 2014, *Sub-millimeter measurement of finite strains at cutting tool tip vicinity,* Experimental Mechanics, Society for Experimental Mechanics, 54(6): 1031-1042.

H. **Puls**, F. Klocke, D. Lung, 2014, *Experimental investigation on friction under metal cutting conditions*, Journal of wear, 310 : 63-71.

*D. **Soler**, P. X. Aristimuño, A. Garay, P. J. Arrazola, 2015, Uncertainty of Temperature Measurements in Dry Orthogonal Cutting of Titanium Alloys,* Journal of Infrared Physics and Technology.

*D. **Soler**, P. X. Aristimuño, M. Saez de Buruaga, A. Garay, P. J. Arrazola, 2018, New Calibration method to measure Rake Face Temperature of the tool during Dry Orthogonal Cutting using Thermography,* Applied Thermal Engineering.

G. **Sutter**, A. Molinari, L. Faure, J.R. Klepaczko, D. Dudzinski, 1998, *An experimental study of high speed orthogonal cutting*, Journal of manufacturing science and engineering, vol 120/171.

G. **Sutter**, L. Faure, A. Molinari, N. Ranc, V. Pina, 2003, *An experimental technique for the measurement of temperature fields for the orthogonal cutting in high speed machining*, International journal of machine tools & manufacture, 43: 671-678.

**Ferrand Controls Inductosyn :** (https://www.cti.fr/national/capteurs-de-position)

B. **Thimm**, M. Reuber, 2018, *Experimental strategies to retrieve data for FEA material models in metal cutting*, European Users Conference 2018.

Q. **Wang**, Z. Liu, B. Wang, Q. Song, Y. Wan, 2015, *Evolutions of grain size and micro-hardness during chip formation and machined surface generation for Ti-6Al-4V in high-speed machining*, International journal of advanced manufacturing technology.